MUSCLE DIFFRACTION THEORY

Relationship between Diffraction Subpeaks and Discrete Sarcomere Length Distributions

M. M. JUDY, V. SUMMEROUR, T. LECONEY, R. L. ROA, AND G. H. TEMPLETON
Departments of Physiology and Medical Computer Science, University of Texas Health Science Center at Dallas, Dallas, Texas 75235; Baylor University Medical Center, Dallas, Texas 75246

ABSTRACT A theoretical discussion is presented that describes the diffraction on monochromatic light by a three-dimensional sarcomere array having the following properties. The basic repetitive diffracting unit is the sarcomere. The contiguous arrangement of physically attached serial sarcomeres in the myofibril is contained within the model so that relative positions of sarcomeres depend upon the lengths of intervening ones. Sarcomere length is described by a distribution function. This function may be discrete or continuous and contain one or more subpopulations. Two arrangements of sarcomeres are considered: (*a*) when sarcomeres of different lengths are arranged randomly in myofibrils the amplitude and width of *m*th order ($m \geq 1$) peaks and associated secondary diffraction maxima decrease and increase monotonically, respectively, as the standard deviation of the length distribution increases. No subpeaks are present regardless of the number of subpopulations within the distribution function. This behavior is shown to follow from the dependence of sarcomere position on the length of intervening sarcomeres. (*b*) When sarcomeres belonging to the same length subpopulation are arranged in serial contiguous fashion to form domains and more than one length subpopulation is present, then *m*th order diffraction peaks split to form subpeaks. The theoretical basis for this behavior is developed for the first time and may explain the subpeaks evident in diffraction patterns from cardiac and skeletal muscle.

INTRODUCTION

The A and I bands of the basic unit of striated muscle, the sarcomere, have different protein concentrations (1, 2), and hence different optical refractive indices. Optically, striated muscle consists of a three-dimensional quasi-periodic array of alternating regions of different refractive indices. Muscle therefore behaves as a three-dimensional diffraction grating. To measure sarcomere function, specific diffraction theory has been developed to determine both average sarcomere length (1–6) and the distribution of sarcomere length (2, 5, 7). This theory is based on the assumption that all sarcomeres within the muscle volume exposed to a laser beam have lengths that vary about the mean and are randomly distributed within the array, regardless of length. The validity of the previous theory has been based on the reported agreement between these sarcomere parameters as determined by diffractometry and light microscopy (3, 5, 7).

However, there are limitations to any diffraction theory that is based upon the assumption that sarcomeres of different lengths are randomly distributed throughout the array. Published diffraction patterns from skeletal and cardiac muscle frequently exhibit subpeaks at positions other than that corresponding to the mean value of sarcomere length. These subpeaks are forbidden in patterns from an array of diffracting elements having randomly distributed spacing. Subpeaks have also been noted in diffraction patterns obtained from skeletal muscle at rest (8, 9). As observed in diffraction patterns from contracting skeletal muscle (1, 5) and isolated single heart cells (10), these subpeaks develop during a contraction by the splitting of the first-order diffraction peak. In addition, these subpeaks have been observed to evolve during contraction of atrial strands after severe passive stretching (3).

Working from fundamental diffraction theory, we have derived equations that predict the effects on light diffraction, caused by periodic and nonperiodic aberrations in the regular spacing of the sarcomeres and myofilaments. These spacing aberrations alter the diffraction pattern by influencing both the average refractive index (scattering power) of the sarcomeres and the wave interference of light diffracted by all sarcomeres. Our equations include the influences of these two factors. Computer generated diffraction patterns obtained from our equations more closely approximate actual patterns from muscle than do patterns predicted from a perfectly uniform array. Specifically, our theoretical patterns demonstrate both the shorter, wider peak shape and the subpeaks which are characteristic of published diffraction patterns and which are not

predicted in diffraction patterns from uniform arrays. Additionally, this theory shows that the subpeaks are present only if (*a*) the sarcomere length population distribution is multimodal, i.e., has two or more discrete length populations and (*b*) serially contiguous sarcomeres of the same length population are clustered together within myofibrils to form domains.

This new theory has potential application in the explanation of subpeaks in diffraction patterns from cardiac and skeletal muscle and in the quantification of changes in the sarcomere length population that may occur in the contractile process.

We have used fundamental diffraction theory to develop equations that uniquely relate structural features of the three-dimensional sarcomere array to important measurable properties of the diffraction pattern, such as peak location, height, and width.

LIST OF SYMBOLS

The symbols are arranged under the headings of the section of text within which they are introduced.

Sarcomere Array

$\hat{\mathbf{i}}, \hat{\mathbf{j}}, \hat{\mathbf{k}}$ Unit vectors directed parallel to the x', y', z' coordinate axes within the sarcomere array. k defines the direction of the myofibrillar axis.

j Index denoting one of $2J$ sarcomeres within a myofibril.

mn Pair of indices denoting one of the $(2M + 1)(2N + 1)$ myofibrils within the array. The index $\pm n$ indicates counting in a direction parallel to the $\pm y'$ axis.

L_{jmn} Length of the jmnth sarcomere.

$\bar{R}_{jmn}$ Position vector of the jmnth sarcomere (Eq. 1). Its components parallel to i, j, h are $R_{x'jmn}$, $R_{y'jmn}$, and $R_{z'jmn}$, respectively (Eqs. 2–5).

ΔZ_{mn} Z-disk misregistry of the mnth myofibril measured relative to the $y'z'$ plane.

Sarcomere Length Distribution

For the entire length distribution:

$H(L)$ Length distribution function for all sarcomeres within the array.

L_0 Mean length of sarcomeres belonging to $H(L)$.

σ Standard deviation of the lengths of sarcomeres belonging to $H(L)$.

M Number of subpopulations comprising $H(L)$.

For the μth subpopulation of $H(L)$ where $1 \leqq \mu \leqq$ M:

$h_\mu(L)$ length distribution function for the μth subpopulation.

g_μ Number fraction of sarcomeres comprising $h\mu(L)$. Sum of all g_μ equals unity.

$L_{0\mu}$ Mean length of sarcomeres comprising $h_\mu(L)$.

σ_μ Standard deviation of the lengths of sarcomeres making up $h_\mu(L)$.

For the qth domain of contiguous serial sarcomeres belonging to the same subpopulation:

$h_q(L)$ Length distribution function for the K_q sarcomeres comprising the domain. If the number K_q accounts for all sarcomeres in $h_\mu(L)$, then $h_q(L) = h_\mu(L)$. If not, then the members of $h_\mu(L)$ are disbursed over q, q', . . . domains and the sum of the corresponding $h_q(L)$ equals $h_\mu(L)$.

K_q Number of contiguous serial sarcomeres clustered together to form the qth domain and comprising $h_q(L)$.

L_{0q} Mean length of sarcomeres belonging to $h_q(L)$.

σ_q Standard deviation of the lengths of sarcomeres belonging to $h_q(L)$.

Geometry of the Diffraction Equipment

E_0 The amplitude of the incident optical electrical field.

λ Wavelength of incident light in vacuum.

n_0 Average optical refractive index of muscle.

R_0 Distance between sarcomere array and plane of the detector.

$\bar{\mathbf{s}}_0$ Incident light vector parallel to the unit vector $\mathbf{j}$ with magnitude $(2\pi n_0/\lambda)$.

$\bar{\mathbf{s}}$ Scattered light vector having components parallel to $\mathbf{i}$, $\mathbf{j}$, $\mathbf{k}$ and defined by Eq. 6.

Diffracted Light Intensity

$\delta L, \delta L_q, \delta L_p$ Fluctuations in length about the mean of the length population $H(L)$ and subpopulations $h_q(L)$ and $h_p(L)$.

E The diffracted electrical field (Eq. 7).

f_{jmn} Scattering function describing pattern of light intensity diffracted by a single sarcomere (Eq. 9) jmn dropped for convenience in subsequent equations.

$f_a f_b$ Scattering functions for the A- and I-bands respectively which are defined by integrals analogous to Eq. 9 for the sarcomere.

f_0 Scattering function for sarcomere of average length L_0.

F_{mn} Interference function given by Eq. 14, which describes the effect on the diffracted electrical field arising from phase differences in light diffracted by all sarcomeres located at their positions within the myofibril.

$\langle \text{Function}(L) \rangle_L^K = [\text{Function}(L_0)]^k \cdot \langle \text{Function}(\delta L) \rangle_{\delta L}^k$ Angular brackets denote averages of the enclosed function over the subscripted quantity; superscripts denote raising the average to the indicated power.

$\langle |F_{mn}|^2 \rangle_L : L \langle |F|^2 \rangle_L$ Averages over length of the square of the absolute magnitude of the interference function (Eqs. 15–34).

$\langle F_{mn} \rangle_L \langle F^*_{m'n'} \rangle_L$ Product of the average over length of the interference function (Eq. 15–35).

$\langle f \rangle_L$ Average over length of the sarcomere scattering function (Eqs. 21 and 22).

$\langle |f|^2 \rangle$ Average over length of the square of the absolute magnitude of the sarcomere scattering function.

$\langle G(R_{y'}, R_{z'}, \Delta Z) \rangle$ Interference function given by Eqs. 16 and 17 which describes the effects on diffracted light intensity due to all myofibrils with different lateral positions.

I The diffracted light intensity given by Eq. 15–35.

$\mathcal{L}_{jmn}$ Sum of lengths of all sarcomeres located between $j = 1$ and $j = j'$ within a single myofibril.

$[n(r) - n_0]$ Dependence on position r of the refractive index within a single sarcomere.

$\bar{\mathbf{S}}$ The scattering vector defined by Eq. 8 as the vector difference between the incident light vector $\bar{\mathbf{s}}_0$ and scattered light vector $\bar{\mathbf{s}}$.

SARCOMERE ARRAY

Our model of the diffracting sarcomere array is based upon structural and optical properties of striated muscle. Except for our introduction of a sarcomere length distribution, it is similar to that used in the theoretical study by

Yeh and co-workers (12) and is shown in Fig. 1. We will consider an array of parallel myofibrils with their axes located perpendicular to the direction of the incident light or optical axis. The array is taken to be centered upon the $x'y'z'$ coordinate system with the myofibrillar axis parallel to the x' axis. This placement is entirely arbitrary and is used here for convenience in defining indices. The indices are used in subsequent summations of the contributions to diffraction by all sarcomeres in order to arrive at the total diffracted optical electrical field and light intensity. The number of myofibrils lying in a direction parallel to the incident light beam is $2N + 1$; the number occurring in the direction perpendicular to both the myofibrillar and optical axes (i.e., across the width of the muscle) is taken to be $2M + 1$. Each myofibril within the region illuminated by the beam contains serially arranged sarcomeres, $2J$ in number. Each sarcomere of the array is labeled by the sequence of integer indices jmn, where $-J \leqq -j \leqq -1$ and $1 \leqq j \leqq J$, denote any sarcomere lying respectively in the half-spaces containing the negative and positive x'-axis. Similarly, the absolute values of both m and n lie in the range $0 \leqq |m| \leqq M$ and $0 \leqq |n| \leqq N$, respectively, and the algebraic sign of the index identifies the half-space relative to y'- and z'-axes within which the sarcomeres are located. The z-disk occurring between the sarcomeres labeled -1, 0, 0 and 1, 0, 0 is located at the origin. All $2J$ sarcomeres having $m = n = 0$ lie within the myofibril directed along the x'-axis.

Examination of Fig. 1 shows that parallel myofibrils in this model are packed into planes extending in directions parallel to both the y'- and z'-axes. The spacing between any pair of adjacent myofibrils in a direction parallel to the y'-axis is labeled Y and that in a direction parallel to the z'-axis is labeled Z.

The plane defined by the z-disks of all sarcomeres labeled $1mn$ (or, equivalently, $-1mn$) will display the contour of the z-disk misregistry of the array relative to the $y'z'$ plane. The z-disk misregistry of the sarcomeres in the mnth myofibril is defined as Δz_{mn}. Relative to the $Y'Z'$ plane, any Δz_{mn} may be algebraically positive or negative.

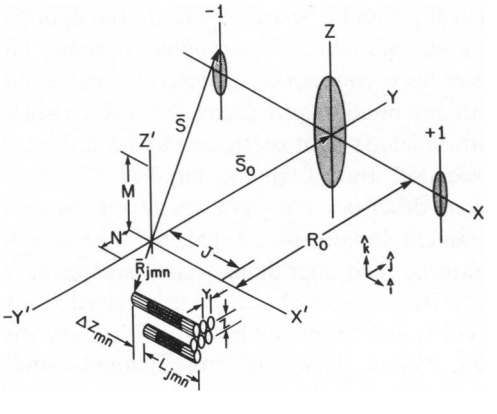

FIGURE 1 The three-dimensional sarcomere array and diffraction pattern used in the derivation of light diffraction equations.

The length of the jth sarcomere in the mnth myofibril is denoted by the symbol L_{jmn}. Because the serially arranged sarcomeres within each myofibril are contiguous, the distance from the z-disk existing between the sarcomeres labeled $-1 = m, n$ and $1 = m, n$ to the z-disk of the j, m, nth sarcomere is equal to the sum of the lengths of all intervening sarcomeres within the myofibril. Thus, although generally the length of each sarcomere L_{jmn} may be independent of all other sarcomere lengths, its position relative to the z-disk misregistry contour is not.

The position of each sarcomere labeled j, m, n, relative to the origin is described by the radius vector $\mathbf{R}_{jmn}$, which is directed from the origin to the sarcomere as shown in Fig. 1. In terms of components parallel to each of the $x'y'z'$-axes,

$$\bar{\mathbf{R}}_{jmn} = R_{x'jmn}\hat{\mathbf{i}} + R_{y'jmn}\hat{\mathbf{j}} + R_{z'jmn}\hat{\mathbf{k}}, \tag{1}$$

where for uniform spacing between myofibrils,

$$R_{y'jmn} = nY + \tfrac{1}{2}Y \tag{2}$$

$$R_{z'jmn} = mZ \tag{3}$$

and

$$R_{x'jmn} = \Delta Z_{mn} \pm L_{1mn} \pm L_{2mn} \pm \ldots \pm L_{(j-1)mn} \tag{4}$$

in which the algebraic sign denotes a sarcomere located in the positive or negative half-spaces separated by the $y'z'$ plane. For $j \geqq 2$,

$$R_{x'jmn} = \Delta Z_{mn} \pm \sum_{k=1}^{j-1} L_{(k-1)mn}, \tag{5}$$

in which the quantity summed over the dummy index k is the distance along the mnth myofibril between the j, m, n-th sarcomere and the z-disk lying between the sarcomeres labeled $-1, m, n$ and $1, m, n$. This z-disk lies within the contour of the z-disk misregistry of the array.

The sarcomeres lying within the diffracting array will be considered to have a length distribution. This distribution $H(L)$ is generally considered to consist of a set of discrete subpopulations, M in number, and to have mean length L_0 and standard deviation σ. Each subpopulation $h_\mu(L)$ has a characteristic mean length $L_{0\mu}$ and dispersion about the length specified by the standard deviation σ_μ. Additionally each subpopulation is occupied by a specific number fraction g_μ of the total number of sarcomeres in the array. The g_μ are constrained by $0 \leqq g_\mu \leqq 1$ and are interdependent through the restriction that the sum of all g_μ for $1 \leqq \mu \leqq M$ must equal unity. Additionally the sum of all $g_\mu L_{0\mu}$ equals L_0. A special case of a subpopulation arises if K_q serial contiguous sarcomeres ($1 \leqq K_q \leqq 2J$) within a myofibril belong to the same length subpopulation $h_q(L)$. This group of sarcomeres defines a sarcomere domain q. All sarcomeres within each domain, therefore, have lengths distributed about the characteristic mean length L_{0q} with standard deviation σ_q. In general, any myofibril

may contain more than one domain, each having K_q sarcomeres with the constraint that the sum of all K_q must not exceed $2J$. Additionally, if they are not serially contiguous, then more than one domain may have the same characteristic mean length L_{0q}. If this is the case for domains labeled $q, q', \ldots$ then the sum of the $h_q(L)$, $h_{q'}(L)$, ... is equal to the subpopulation $h_\mu(L)$. The total number of sarcomeres within this subpopulation is equal to the sum of the $K_q, K_{q'}, \ldots$. The standard deviation σ_μ is equal to the sum of the $\sigma_q, \sigma_{q'}, \ldots$. Domains containing sarcomeres belonging to the same $h_\mu(L)$ may be located either within a single myofibril or within different ones.

Geometry of the Diffraction Experiment

For recording optical diffraction patterns from muscle, the sarcomere array and detector are usually placed, relative to each other, at a distance R_0 along the y-axis as shown in Fig. 1. Incident light of wavelength λ, electrical field amplitude E_0, and wave vector $\bar{s}_0 = (2\pi n_0/\lambda)j$ is directed along the y-axis and is incident normally upon the sarcomere array. The quantity n_0 is the average index of refraction of the muscle. The scattered light vector $\bar{s}$ is parallel to the direction of the diffracted light and is given by

$$\bar{s} = (2\pi n_0/\lambda)(\alpha\hat{i} + \beta\hat{j} + \gamma\hat{k}) \tag{6}$$

where α, β, γ are direction cosines relative to the cartesian coordinates x, y, z. The plane of the detector usually coincides with the xz-plane of this coordinate system. The unit vectors $\hat{i}, \hat{j}, \hat{k}$ define a right-handed set with $\hat{i}$ typically parallel to the x- or x'-axis.

The mutually perpendicular meridional and equatorial axes of the diffraction pattern lie within the detector plane with the meridional axis oriented along the x-axis. Thus, the meridional axis is parallel with the myofibrillar axis. Typically, recorded diffraction patterns from muscle show peaks arrayed with equal spacing along the meridional axis.

In most muscle optical diffraction experiments the distance R_0 between the preparation and the plane of the detector is very large compared with both the wavelength of the incident light and the mean characteristic spacing of the diffracting array. These relationships suggest that under these experimental conditions a Fraunhoffer diffraction pattern (13) will be present and that the Kirchoff's scalar field theory (14) will permit the amplitude of the diffracted electrical field at the detector to be closely approximated.

DIFFRACTED LIGHT INTENSITY

The intensity of diffracted light measured at any point on the surface of the detector is equal to the square of the amplitude of the optical electrical field formed by the scattering of the incident field by all sarcomeres within the array.

In the framework of Kirchoff scalar field theory (14) the amplitude of the diffracted electrical field E is obtained by summing the contribution made to the field by each sarcomere with regard for its phase which is dependent on the position of the sarcomere within the array.

$$E = \sum_{jmn} f_{jmn} \exp(i\bar{S} \cdot \bar{R}_{jmn}) \tag{7}$$

where $i = -1$ and the sum extends over all sarcomeres labeled jmn and the scattering vector $\bar{S}$ is given in terms of the scattered light vector $\mathbf{s}$ (Eq. 6) and the incident light vector $\mathbf{s}_0$ by

$$\bar{S} = \bar{s} - \bar{s}_0. \tag{8}$$

The scattering amplitude, f_{jmn}, describes the angular variation in the intensity of the light diffracted by a single sarcomere through the equation

$$f_{jmn} = \frac{E_0}{4\pi R_0 V_{jmn}} \exp(i|\bar{S}_0|R_0) \int [n(r') - n_0]_{jmn} \exp(i\bar{S} \cdot \bar{r}'_{jmn}) dV_{jmn}, \tag{9}$$

where $|\bar{s}_0|$ is the magnitude of $\bar{s}_0$ and the integration extends over the volume V_{jmn} of the sarcomere and the term, $[n(r) - n_0]_{jmn}$ describes the dependence of the refractive index on its position ($\bar{r}'_{jmn}$) within the sarcomere. If this quantity were zero, thus indicating a homogeneous refractive index over the myofibril volume, the scattering amplitude would be zero and the incident beam would pass through the tissue without being attenuated in amplitude and without any angular spread. As shown by Hanson and Huxley (2), the thick and thin filament bundles and the z-plate comprise discrete regions having different protein concentration and different refractive indices. Their relative positions define the term $[n(r) - n_0]$ in Eq. 9. With this model the integral of Eq. 9 can be rewritten (4, 15) as

$$\mathcal{J}_{jmn} = f_a + f_b \exp(iS_x L_{jmn}/2), \tag{10}$$

where S_x is the x-component of the scattering vector defined in Eq. 8 and where f_a and f_b are the light scattering functions for these discrete sarcomere regions. The quantity f_a has been considered to describe scattering by the thin filament bundles projecting from the z-disk (4, 15) and to also include light scattering by both the z-disk and two associated thin filament bundles (7, 12, 16). The quantity f_b describes the light scattering pattern of the thick filament bundle (4, 12, 15, 16). The equations for the equatorial and meridional light scattering patterns obtained with cylindrical scatterers, derived by Bear and Bolduan (17), have been applied (4, 12, 15, 16) to describe scattering by the thick and thin filament bundles. The imaginary exponential in Eq. 9 takes into account differences in phase resulting from spatially separated regions having different optical refractive indices.

The argument of each exponential term in the sum of Eq. 7 is the phase shift in the incident light wave $\bar{s}_0$ introduced by scattering from the *jmn*-th sarcomere. The phase for each sarcomere is seen to depend on the scattering vector $\bar{S}$ in Eq. 8, and the position vector $\bar{R}_{jmn}$, defined previously.

The diffracted light intensity, I, from a quasi-periodic array can be written as described by Born and Wolf (18):

$$I = \langle |E|^2 \rangle \tag{11}$$

where the brackets denote an average value and E is given by Eq. 7. The mathematical process of averaging $|E|^2$ (by integration over the distribution function describing fluctuations in periodicity) gives the measured light intensity as the sum of: (*a*) the light intensity diffracted (coherently scattered) by the ideal periodic array with mean values of spacing and (*b*) the light intensity incoherently scattered by deviation by the array from periodic values.

Let the equations

$$\begin{aligned} S_x &= \bar{S} \cdot \hat{i} \\ S_y &= \bar{S} \cdot \hat{j} \\ S_z &= \bar{S} \cdot \hat{k} \end{aligned} \tag{12}$$

define the cartesian components of the scattering vector $\bar{S}$ in Eq. 8 and

$$\mathcal{L}_{jmn} = \sum_{k-1}^{j-1} L_{(k-1)mn} \tag{13}$$

and

$$F_{mn} = \sum_{j=-J}^{J} f_{jmn} \exp\left(iS'_x \mathcal{L}_{jmn}\right) \tag{14}$$

define the effect on the phase of the optical electrical field. Substitution of Eq. 7 for the scattered optical electrical field into Eq. 11 gives for the diffracted light intensity I in terms of F_{mn}

$$\begin{aligned} I = \frac{E_0^2}{16\pi^2 R_0^2} \Bigg(& \sum_{m=-M}^{M} \sum_{n=-N}^{N} \langle |F_{mn}|^2 \rangle_L \\ & + \sum_{m=-M}^{M} \sum_{n=-N}^{N} \sum_{m'=-M'}^{M'} \sum_{n'=-N'}^{N'} \{ \langle \exp [i[S_y(R_{y'mn} - R_{y'm'n'}) \\ & + S_{z'}(R_{z'mn} - R_{z'm'n'}) \\ & + S_x(\Delta Z_{mn} - \Delta Z_{m'n'})]] \rangle_{y',z',\Delta z} \langle F_{mn} \rangle_L \langle F^*_{m'n'} \rangle_L \\ & + \langle \exp \{-i[S_{y'}(R_{y'mn} - R_{y'm'n'}) + S_z(R_{z'mn} - R_{z'm'n'}) \\ & + S_x(\Delta Z_{mn} - \Delta Z_{m'n'})]] \rangle_{y',z',\Delta z} \langle F^*_{mn} \rangle_L \langle F_{m'n'} \rangle] \Bigg) \end{aligned} \tag{15}$$

where, in the second sum, $m \neq m'$, and $n \neq n'$ and the index j has been dropped from the position vector components R as all sarcomeres within a myofibril are considered to be coaxial. For both summations, the subscripts of the angular brackets denote averages of the enclosed quantities over the corresponding distribution functions. The asterisk notation F^* denotes the complex conjugate of the function F. Eq. 15 is a general statement relating the diffracted light intensity to the structural parameters of the diffracting sarcomere array and their spatial arrangement.

The first term of Eq. 15 containing the quantity $|F_{mn}|^2$ describes the light intensity diffracted by sarcomeres within the *mn*-th individual myofibril. Averaging all terms for all *mn* sarcomeres over the length distribution $H(L)$ and summing over all m and n gives the contribution of the average myofibril to the light intensity. Since F_{mn} is dependent only upon $(S_x \mathcal{L}_{jmn})$ (as shown by Eq. 14) and is not dependent upon $S_y R_{y'mn}$, $S_Z R_{z'mn}$, and $S_x \Delta Z_{jmn}$, the diffracted light intensity due to the average myofibril lies entirely along the meridional axis.

The quantity $F_{mn}F_{m'n'}$ found in the second term of the sum comprising Eq. 15 describes the diffracted light intensity arising from wave interference between light scattered by sarcomeres in the pair of different myofibrils labeled *mn* and *m'n'*. Averaging all terms $F_{mn}F_{m'n'}$ over the length distribution and summing over all values of m, m', n, n' (as described by Eq. 15) gives the contribution of the average pair of myofibrils to the light intensity. As shown by Eq. 15, the light intensity arising from the average pair of myofibrils is weighted by terms that depend upon the transverse structural parameters $(R_{y'mn} - R_{y'm'n'})$ and $(R_{z'mn} - R_{z'm'n'})$ and upon z-disk misregistry (ΔZ_{mn}). The contribution from these structural parameters and from z-plate misregistry (12, 19) can profoundly affect the contribution of the average pair of myofibrils to the meridional diffraction pattern. Because the contribution by the average pairs of myofibrils is given by $(2M + 1)(2N + 1)[(2M + 1)(2N + 1) - 1]$ terms, the contribution of this pair is potentially much larger, and hence more important, in establishing the meridional diffraction pattern than the contribution by the average myofibril which contains only $(2M + 1)(2N + 1)$ terms.

The general Eq. 15 for the diffracted light intensity can be simplified if the spatial distribution of sarcomeres, which belong to $H(L)$ because of their lengths, is homogeneous over the volume of myofibrils within $(2N + 1)(2M + 1)(2J)$. In this case a segregation of myofibrils containing sarcomeres belonging to different subpopulations of $H(L)$ will not occur. Accordingly, $\langle F_{mn} \rangle \langle F^*_{m'n'} \rangle$ and its complex conjugate are equal, and can be factored from the quadruple sum. Additionally, $\langle |F_{mn}|^2 \rangle$ can be factored from the double sum, and Eq. 15 written as

$$\begin{aligned} I = \frac{E_0^2}{16\pi^2 R_0^2} & \{2M + 1)(2N + 1)\langle |F|^2 \rangle_L \\ & + \langle F \rangle_L \langle F^* \rangle_L \langle G(y', z', \Delta z) \rangle_{y',z',\Delta z} \end{aligned} \tag{16}$$

where

$$\langle G(y', Z', \Delta Z)\rangle_{y',z',\Delta z} = 2\sum_{m=-M}^{M}\sum_{n=-N}^{N}\sum_{m'=-M'}^{M'}\sum_{n'=-N'}^{N'} \cdot \langle \cos[S_y(R_{y',m} - R_{y'm'n'}) + S_z(R_{z'mn} - R_{z'm'n'}) + S_x(\Delta Z_{mn} - \Delta Z_{m'n'})]\rangle_{y',z',\Delta z} \quad (17)$$

in which $m \neq m'$ and $n \neq n'$. In Eq. 16, fluctuations in the lateral spacing, $R_{y'mn}$ and $R_{z'mn}$, between myofibrils are considered to be independent of fluctuations in sarcomere length. Additionally, all $2J$ sarcomeres within each myofibril are taken to be coaxial, so that the mean values of the lateral spacing, Y_{0mn} and Z_{0mn}, and fluctuations about the mean are both ascribed to an entire myofibril. The terms

$$\langle |F|^2\rangle_L = \left\langle \sum_{j=-J}^{J} f_j e^{ijS_x\mathcal{L}_j} \sum_{j=-J}^{J} f_j^* e^{-ijS_x\mathcal{L}_l}\right\rangle_L \quad (18)$$

and

$$\langle F\rangle_L\langle F^*\rangle_L = \left\langle \sum_{j=-J}^{J} f_j \exp(ijS_x\mathcal{L}_j)\right\rangle_L \left\langle \sum_{j=-J}^{J} f_j^* \exp(-ijS_x\mathcal{L}_j)\right\rangle_L, \quad (19)$$

which appear in Eq. 16 explicitly show that the light intensity diffracted by the average myofibril $\langle |F|^2\rangle$, and by the average pair of myofibrils $\langle F\rangle\langle F^*\rangle$ depends solely upon sarcomere length and the distribution of this parameter. The indicated averages in Eqs. 18 and 19 over the length distribution account for the effects of aberrations in the periodicity of sarcomere length on the meridional diffracted light intensity. These averages are considered in the present work. The quantity $\langle G\rangle$ given by Eq. 17 accounts for the effects on the meridional diffracted light intensity which arise from two factors: (*a*) the three-dimensional nature of the sarcomere array as emphasized by Rudel and Zite-Ferenczy (9) and by Yeh et al. (12) and (*b*) fluctuations about mean values of both the lateral myofibrillar spacing and the *z*-plate misregistry contour (12). The following analysis in this paper will also consider the first factor, while the effects on the second will be considered in a future publication.

The form of equations for $\langle |F|^2\rangle$ and $\langle F\rangle_L\langle F^*\rangle_L$ obtained from averaging over the sarcomere length distribution depends upon the mathematical form of $H(L)$ and on whether sarcomeres of different lengths within the population are arranged in a random sequence or in serial contiguous sarcomere domains containing members of the same sarcomere length.

Case I

Sarcomeres Arranged in Random Sequence. If the lengths of all serial sarcomeres in all myofibrils *mn* are arranged randomly, then the expressions for the intensity of the light diffracted by both the average myofibril and the average pair of myofibrils are given by

$$\langle |F|^2\rangle = \Bigg\{2J\langle |f|^2\rangle_L + \sum_{j=1}^{2J-1}(2J-j)\Bigg[\langle f\rangle_L\left\langle f^*\exp\left(iS_x\frac{L}{2}\right)\right\rangle_L \cdot \langle \exp(iS_x'L)\rangle_L^{j-1/2} + \langle f^*\rangle_L\left\langle f\exp\left(-iS_x\frac{L}{2}\right)\right\rangle_L \cdot \langle \exp(-iS_xL)\rangle_L^{j-1/2}\Bigg]\Bigg\} \quad (20)$$

and

$$\langle F\rangle\langle F^*\rangle = \langle f\rangle_L\langle F^*\rangle_L\Bigg\{2J + \sum_{j=1}^{2J-k-1}\sum_{k=0}^{2J-2} \cdot [\langle \exp(-iS_xL)\rangle_L^k\langle \exp(iS_xL)\rangle_L^{j+k} + \langle \exp(iS_xL)\rangle_L^k \langle \exp(-iS_xL)\rangle_L^{j+k}]\Bigg\}. \quad (21)$$

Terms in Eqs. 20 and 21 which depend upon the intensity of the light scattered by the sarcomere given by Eq. 10 and averaged over $H(L)$ are given by

$$\langle f\rangle_L\left\langle f^*\exp\left(iS_x\frac{L}{2}\right)\right\rangle_L = \left[\left(f_a + f_b\left\langle \exp\left(iS_x\frac{L}{2}\right)\right\rangle_L\right) \cdot \left(f_a\left\langle \exp\left(iS_x\frac{L}{2}\right)\right\rangle_L + f_b\right)\right] \quad (22)$$

$$\langle |f|^2\rangle = f_a^2 + f_b^2 + f_af_b\left(\left\langle \exp\left(iS_x\frac{L}{2}\right)\right\rangle_L + \left\langle \exp\left(-iS_x\frac{L}{2}\right)\right\rangle_L\right) \quad (23)$$

and

$$\langle f\rangle\langle f^*\rangle = \left[f_a + f_b\left\langle \exp\left(iS_x\frac{L}{2}\right)\right\rangle_L\right] \cdot \left[f_a + f_b\left\langle \exp\left(-iS_x\frac{L}{2}\right)\right\rangle_L\right]. \quad (24)$$

In taking averages over $H(L)$ in Eqs. 22–24, we have omitted for convenience the dependence of sarcomere diameter and, consequently, the thick and thin filament bundle diameters on sarcomeres length. Since bundle diameter enters only into the radial scattering function, [e.g. Bear and Bolduan (17)] and this function is approximately unity in the vicinity of the meridional axis, this approximation will not affect the present examination of the effect of sarcomere length distribution on meridional diffracted light intensity.

Averages over $H(L)$ can be written in terms of the distribution of fluctuation in length δL, about the mean value L_0, to give

$$\langle \exp(iS_x L)\rangle_L^k = \langle \exp(iS_x \delta L)\rangle_{\delta L}^k \exp(ikS_x L_0) \quad (25)$$

where $\langle \exp(iS_x \delta L)\rangle_{\delta L}$ is mathematically equivalent to the Fourier transform of the distribution function $H(\delta L_{mn})$ (20). According to the central limit theorem (21), for any physically realistic $H(\delta L_{mn})$ (which implies that the integral

$$\int L^{\alpha} H(L)\mathrm{d}L \quad (26)$$

for $\alpha \geqq 2$ is bounded) the Fourier transform of the distribution function, raised to any power k, can be written as a gaussian function,

$$\langle \exp(iS_x \delta L)\rangle_{\delta L}^k = \exp(-kS_x^2 \sigma_{mn}^2 | 2), \quad (27)$$

where σ_{mn} is the standard deviation of $H(\delta L_{mn})$. Thus, any periodic variations in $\langle \exp(iS_x \delta L)\rangle$ that might be present and contribute a phase angle term to $\exp(ikS_x L_0)$ are damped out. These variations would arise if (*a*) the distribution is multimodal, i.e., containing more than one subpopulation or (*b*) if the distribution function is mathematically assymetric about L_0. Because these variations are damped, subpeaks do not form. Therefore, detailed information about both the presence of discrete subpopulations, and the mathematical form of the distribution function, are not present in the diffraction pattern if the sarcomeres of different lengths are randomly positioned within the array. The only information available in the diffraction pattern is L_0, which is obtained from the relative locations of the mth order diffractive peaks, and σ, the standard deviation of the length distribution which is obtained from the height and width of the mth order diffraction peak.

To demonstrate the influence of a random array of sarcomeres on the first-order peak of a diffraction pattern, we have obtained computer-generated plots with the use of Eqs. 20 and 21. Parameters for the length distributions shown in Fig. 2 have been used. The distributions for sarcomere length shown in Fig. 2 are for a single gaussian distribution (*A*), and for two discrete multimodal distributions (*B* and *C*). In Fig. 2, the length distribution, $H(L)$, is plotted along the *Y*-axis and sarcomere length (L) is plotted along the *X*-axis. As shown in the figure, the subpopulations, $h(L)$, which comprise discrete length distributions, have heights defined by the number fraction of sarcomeres, g_μ, and, have locations defined by discrete values of sarcomere length, L_μ. The plots for $\langle |F|^2\rangle$ and $\langle F\rangle \langle F^*\rangle$ obtained from Eqs. 20 and 21, shown in Fig. 3, were obtained with omission of the term $\exp(iS_x \delta L/2)$ contained in Eqs. 22–24. The omitted terms are equal to $\exp[S_x^2\sigma^2/8]$ and can be neglected. Given this approximation, the products of terms containing f and its complex conjugate (which can be found in Eqs. 22–24) give f_0^2. This is the scattered light intensity function for the

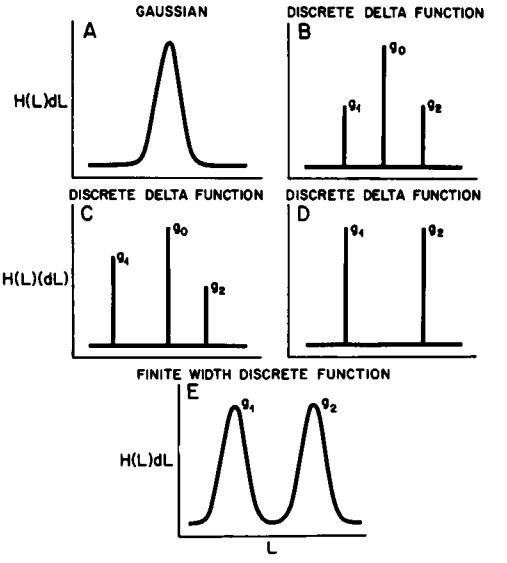

FIGURE 2 Continuous and discrete distributions [$H(L)$] used in modeling the effects of distributed sarcomere length on the meridional diffraction pattern.

sarcomere of average length L_0, which can be factored from the right-hand side of the equations. Diffraction peaks in Fig. 3 show the dependence of the quantities $\langle |F|^2\rangle/f_0^2$ and $\langle F\rangle \langle F^*\rangle/f_0^2$ on the Fourier variable $\omega = S_x L_0$. For this figure and for the computer-generated plots presented subsequently in this paper, values of the standard deviation expressed as a fraction of mean sarcomere length for the various populations $H(L)$ shown in Fig. 2 were taken to be 0, 0.035, and 0.071. These values of

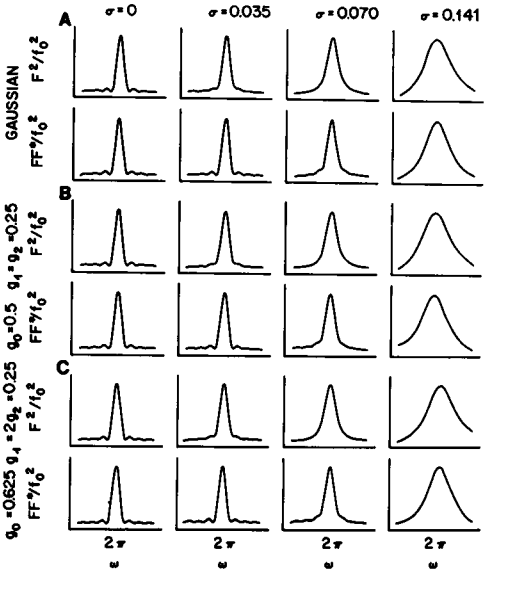

FIGURE 3 First-order diffraction peaks of $\langle |F|^2\rangle/f_0^2$ and $\langle F\rangle \langle F^*\rangle/f_0^2$ computed using Eqs. 20 and 21 for random sarcomere arrays having a continuous gaussian (*A*), symmetrical (*B*) and an assymetrical Dirac delta length distribution function (*C*). The abscissa contains values of the Fourier variable $\omega = S_x L_0$ in the vicinity of $\omega = 2\Pi$.

(σ/L_0) compare in magnitude with values of 0.021 reported for single frog skeletal muscle fibers and values of 0.08–0.10 reported for large bundles of fibers (7).

The mth order diffraction peaks, shown in the plots of Fig. 3, are symmetrical in shape irrespective of both the symmetry of the length distribution, and its discreteness. The maximum of the mth order peak is located, in diffraction or Fourier space, at the position for which $\omega = S_x L_0 = 2m\pi$. Thus, peak location uniquely gives the mean sarcomere length. Additionally, these computer generated first-order peaks exhibit both the monotonic decrease in peak amplitude and the increase in peak width seen with increasing standard deviation σ of the sarcomere length distribution. The first-order diffraction peaks, computed from Eqs. 20 and 21 for $\sigma = 0$, have the amplitude $[(2J)^2]$, and width at the base $[2\Pi/2J)$. This is predicted by the theory which describes the intensity of the light diffracted by a perfectly periodic linear array of diffracting elements (18).

Secondary diffraction maxima are shown in the plots of Fig. 3 to occupy positions adjacent to the major mth order diffraction peaks. These positions satisfy $\omega \simeq (2m + 1)\Pi/4J$. As predicted by the theory of diffraction by a perfect linear array (18) these maxima have amplitudes equal to $4/[2J\pi(2b + 1)]^2$ for $\sigma = 0$, where b is an integer. As the standard deviation of the length distribution increases, the amplitude of these secondary diffraction maxima decrease but their position remains unchanged.

Case II

Sarcomeres Arranged in Domains. Two sarcomere domain arrangements will be considered. In the first arrangement, all of the $2J$ saromeres making up each myofibril are assumed to be a single domain; i.e., they belong to the same subpopulation $h_p(L)$, having characteristic mean length, L_{0p}, population fraction, g_p, and fluctuations about the mean, δL_p. In each myofibril the length of the jth sarcomere $(L_{0p} + \delta L_{pj})$, $1 \leq j \leq 2J$, is assumed to be independent of the length of all other sarcomeres. There are a total of M different subpopulations p.

In the second arrangement, each myofibril, mn, of the array contains Q serial domains. Each domain contains K_q sarcomeres, and is characterized by the subpopulation $h_q(L)$. In this arrangement, K_q summed over q equals $2J$, and in general, $h_q(L) \neq h_{q+1}(L)$ ensures that any two adjacent domains have different characteristic mean length. If domains q and q' are populated from the subpopulation $h_\mu(L)$, then $h_q(L) + h_{q'}(L) = h_\mu(L)$. All δ_{Lq} are taken to be independent.

Arrangement I

Each Myofibril a Domain of 2J Sarcomeres. If each myofibril comprises a domain of sarcomeres having the same mean length L_{0p}, then Eqs. 17 and 18 for $\langle |F|^2 \rangle$ and $\langle F \rangle \langle F^* \rangle$ become

$$\langle |F|^2 \rangle = \Bigg\{ 2J \sum_{p=1}^{p} g_p \langle |f_p|^2 \rangle_{\delta L_p} + \sum_{p=1}^{p} g_p \sum_{j=1}^{2J-1} (J-j) \Bigg[\langle f_p \rangle_{\delta L_p} \left\langle f_p^* \exp\left(iS_x \frac{\delta L_p}{2}\right) \right\rangle_{\delta L_p} \cdot \langle \exp(iS_x \delta L_p) \rangle_{\delta L_p}^{j-1/2} \exp(ijS_x L_{0p}) + \langle f_p \rangle_{\delta L_p} \left\langle f_p \exp\left(-S_x \frac{\delta L_p}{2}\right) \right\rangle_{\delta L_p} \cdot \langle \exp(-iS_x \delta L_p) \rangle_{\delta L_p}^{j-1/2} \exp(-ijS_x L_{0p}) \Bigg] \Bigg\} \tag{28}$$

and

$$\langle F \rangle \langle F^* \rangle = \Bigg\{ \sum_{j=0}^{2J-1} \sum_{p=1}^{p} g_p \langle f_p \rangle_{\delta L_p} \langle \exp(iS_x \delta L_p) \rangle_{\delta L_p}^{j} \sum_{p=1}^{p} g_{p'} \langle f_{p'}^* \rangle_{\delta L_{p'}} \cdot \langle \exp(-iS_x \delta L_{p'}) \rangle_{\delta L_{p'}}^{j} + \sum_{j=1}^{2J-k-1} \sum_{k=0}^{2J-2} \Bigg[\sum_{p=1}^{p} g_p \langle f_p \rangle_{\delta L_p} \cdot \langle \exp(iS_x \delta L_p) \rangle_{\delta L_p}^{j+k} \exp[i(j+k) S_x L_{0p}] \cdot \sum_{p'=1}^{p} g_{p'} \langle f_{p'}^* \rangle_{SL_p} \langle \exp(-iS'_x \delta L_{p'}) \rangle_{\delta L_p}^{k} \cdot \exp(-ikS_x L_{0p'}) + \sum_{p=1}^{p} g_p \langle f_p^* \rangle_{\delta L_p} \cdot \langle \exp(-iS'_x \delta L_p) \rangle_{\delta L_p}^{j+k} \exp[-i(j+k) S_x L_{0p}] \cdot \sum_{p'=1}^{p} g_{p'} \langle f_{p'} \rangle_{\delta L_{p'}} \langle \exp(iS_x \delta L_{p'}) \rangle_{\delta L_{p'}} \cdot \exp(ikS_x L_{0p}) \Bigg] \Bigg\}, \tag{29}$$

where for each subpopulation p the sarcomere scattering factor (Eq. 10) is given by

$$\langle f_p \rangle_{\delta L_p} = f_a + f_b \cdot \left\langle \exp\left(iS_x \frac{\delta L_p}{2}\right) \right\rangle_{\delta L_p} \exp(iS_x L_{0p}/2). \tag{30}$$

Comparison of Eqs. 28 and 20 for the scattering by the average myofibril reveals that for the case where the entire myofibrils comprise a domain, the intensity of the diffracted light is a linear superposition obtained by summations over p, of the light diffracted by g_p myofibrils all of which have mean length L_{0p} and associated $H_p(\delta L)$. Thus, if the sarcomere length distribution function is characterized by mean length L_{01} and L_{02}, the contribution to the meridional diffraction pattern by $\langle |F|^2 \rangle$ will be the weighted sum of the individual diffracted intensities with explicit weighting factors, g_1 and g_2. These intensities will be present as individual subpeaks. Additionally, an

implicit weighting is present through the damping terms $[\exp(iS_x\delta L_p)]^j$. As found in prior discussion of Eqs. 20 and 21, the effect of the damping is to decrease the amplitude and widen the subpeaks.

Comparison of the terms involving products of sums over p and p' in Eq. 29, with terms of Eq. 17, shows that those terms for which $p \neq p'$ do represent a linear superposition of p contributions, each having explicit weighting factor $(g_p)^2$ and each contributing a subpeak. Those terms involving products for which $p \neq p$ also contribute to a linear superposition and have an explicit weighting factor $g_p g_{p'}$. These latter terms contribute only when small phase differences exist between $\delta x L_{0p}$ and $\delta x L_{0p'}$; otherwise these products oscillate between $\pm g_p g_{p'}$, and make a contribution to the intensity which averages to zero.

Computer-generated first-order diffraction peaks for both $\langle |F|^2 \rangle$ and $\langle F \rangle \langle F^* \rangle$, obtained using Eqs. 28 and 29, are shown in Fig. 4. As with our previous computations using Eqs. 20 and 21, the quantity $\exp(s^2\sigma_p^2/8)$ in Eqs. 22–24 has been equated to unity. The results of these computations have been plotted as $\langle |F|^2 \rangle / f_0^2$ and $\langle F \rangle \langle F^* \rangle / f_0^2$ in which f_0 is the scattering function of the sarcomere with length equal to the mean value of the entire length population. The distribution functions $H(\delta L) = \Sigma h_p(L)$ used in these computations are given in Fig. 2.

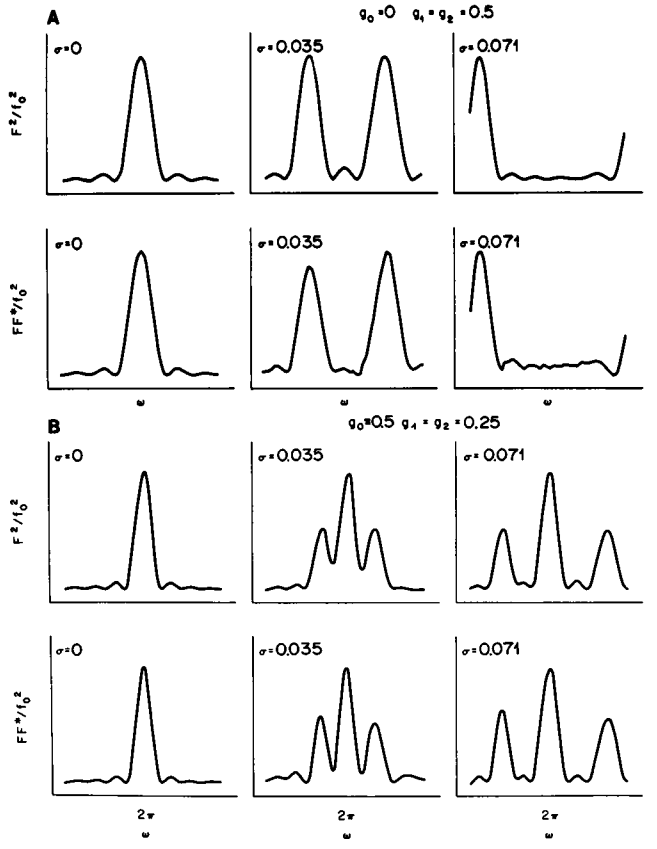

FIGURE 4 First-order diffraction peaks of $\langle |F| \rangle^2 / f_0^2$ and $\langle F \rangle \langle F^* \rangle / f_0^2$ computed using Eqs. 28 and 29 for individual myofibrils comprising domains with sarcomeres of equal length. Each myofibril has characteristic sarcomere length lying within one of the subpopulations of a symmetrical bimodal (A) or trimodal (B) discrete Dirac delta sarcomere length distribution function. These length distributions are shown in Figs. 2 B and D, respectively. The abscissa contains values of the Fourier variable $\omega = S_x L_0$ in the vicinity of $\omega = 2\Pi$.

Arrangement II

Q Serial Domains in Each Myofibril. Each myofibril mn is considered to be made up of Q contiguous serial domains. Each domain contains K_q sarcomeres with mean length L_{0q} and has a distribution of length fluctuations about L_{0p} given by $H_q(\delta L)$. In general, $L_{0q} \neq L_{0q'}$ for all q. The sum of the K_q equals $2J$, and within all myofibrils the sequence of domains q, from $q = 1$ to $q = Q$, is taken to be the same. For this spatial arrangement of sarcomeres,

$$\langle |F|^2 \rangle = \langle F \rangle \langle F^* \rangle \tag{31}$$

with

$$\begin{aligned}
\langle |F|^2 \rangle = \Bigg\{ & \sum_{q-1}^{Q} \Bigg[K_q \langle |f_q|^2 \rangle_{\delta L_q} \\
& + \sum_{k-1}^{k_q-1} (K_q - 1) \Bigg[\langle f_q \rangle_{\delta L_q} \left\langle f_q^* \exp\left(iS_x \frac{\delta L_q}{2}\right) \right\rangle_{\delta L_q} \\
& \cdot \langle \exp(iS_x \delta L_q) \rangle_{\delta L_q}^{k-1/2} \exp(ikS_x L_{0q}) \\
& + \langle f_q^* \rangle_{\delta L_q} \left\langle f_q \exp\left\langle -iS_x \frac{\delta L_q}{2} \right\rangle \right\rangle_{\delta L_q} \\
& \cdot \left\langle \exp\left(-iS_x \frac{\delta L_q}{2}\right) \right\rangle_{\delta L_q}^{k-1/2} \exp(-ikS_x L_{0q}) \Bigg] \\
& + \sum_{p-0}^{Q-q-1} \sum_{q-1}^{Q-1} \Bigg[\sum_{k-1}^{k_q} \langle f_h^* \rangle_{\delta L_q} \\
& \cdot \langle \exp(-iS_x \delta L_q) \rangle_{\delta L_q}^{k} \exp(-ikS_x L_{0q}) \\
& \cdot \sum_{j-1}^{k_{p+q}} \langle f_j \rangle_{\delta L_{p+q}} \langle \exp(iS_x \delta L) \rangle_{\delta L_{p+q}}^{j} \exp(ijS_x L_{0(p+q+1)}) \\
& \cdot \prod_{r-1}^{q+p} \langle \exp(iS_x \delta L) \rangle_{\delta L_r}^{k_r} \exp(iS_x \mathcal{L}_{0(q+p)}) \\
& + \sum_{k-1}^{k_q} \langle f_k \rangle_{\delta L_q} \langle \exp(iS_x \delta L) \rangle_{\delta L_q}^{k} \exp(ikS'_x L_{0q}) \\
& \cdot \sum_{j-1}^{k_{p+q}} \langle f_j^* \rangle_{\delta L_{p+q}} \langle \exp(-iS_x \delta L) \rangle_{\delta L_{p+q}}^{j} \\
& \cdot \exp(-ijS_x L_{0(p+q+1)}) \\
& \cdot \prod_{r-1}^{q+p} \langle \exp(-iS_x \delta L) \rangle_{\delta L_r}^{k_r} \exp(-iS_x \mathcal{L}_{0(q+p)}) \Bigg] \Bigg\},
\end{aligned} \tag{32}$$

where the pi notation denotes

$$\prod_{r-1}^{p+q} x^{k_r} = x^{k_1} x^{k_2} \ldots x^{k_{p+q}} \tag{33}$$

and the quantity

$$\mathcal{L}_{0(q+p)} \equiv \sum_{r=1}^{p+q} K_r L_{0r} \tag{34}$$

with $K_r = 0$ for $r = 1$ in Eqs. 31–34.

Examination of Eq. 30 for $\langle |F|^2 \rangle = \langle F \rangle \langle F^* \rangle$, shows that the single sum over $q = 1$ to Q, is a linear superposition of the meridional diffraction patterns of the Q individual domains and that peak positions are fixed by L_{0q}. The superposition gives rise to subpeaks, which are clustered about the position corresponding to the mean value L_0 of the L_{0q}. The height of each subpeak is weighted explicitly by K_q^2. Therefore, if the δL_q are zero for all q, then the relative heights of subpeaks in $\langle |F|^2 \rangle / f_0^2$, contributed to the single sum over q, will scale as the population fraction. The double sum over indices p and q describes the meridional intensity of light which is diffracted by sarcomeres in different domains. The phase differences, and resulting wave interference, between sarcomers in domains q and q', depend not only upon the relative positions of the sarcomeres within their domains, but also upon the lengths of all intervening domains q'', q''', etc. With $L_{0q} \neq L_{0q'}$, the intensity of the diffracted light due to diffraction effects between sarcomeres in different domains is appreciable only for small differences between the lengths.

Computer generated first-order diffraction peaks for a serial domain model are presented in Fig. 5. As with other computer-generated diffraction peaks presented in this study, the intensity of the diffracted light is presented as $\langle |F|^2 \rangle / f_0^2$. The length distributions shown in Fig. 2 have been used in these computations.

DISCUSSION

We have applied fundamental light diffraction theory (14) to derive equations for the meridional diffraction pattern which results from a three-dimensional array of sarcomeres having a homogeneous length distribution. The equations describe the contributions of both the average myofibril and the average pair of myofibrils due to nonperiodic aberrations in sarcomere length. In addition, the equations describe the effects of clustering of contiguous sarcomeres into domains, each domain having a discrete mean length. The effects on meridional diffraction peak intensity which are described by the present work arise from totally different structural features than those described previously by Yeh and co-workers (12) which were attributed to z-disk misregistry. The equations of Yeh et al. show that random fluctuations, in z-disk alignment within parallel myofibrils, reduce meridional diffraction peak intensity without widening peaks or introducing subpeaks. Equations which they derived for linear misregistry of the z-disk show that this form of misalignment causes meridional diffraction peaks to shift away from the meridional axis, in a direction perpendicular to the axis so that peak intensity of the axis is reduced. However in this scheme no subpeaks are introduced.

Equations derived in the present work show that the presence of both a sarcomere length distribution and the clustering into domains of sarcomeres belonging to the same length subpopulation, have profound effects on both the intensity and the pattern of diffracted light.

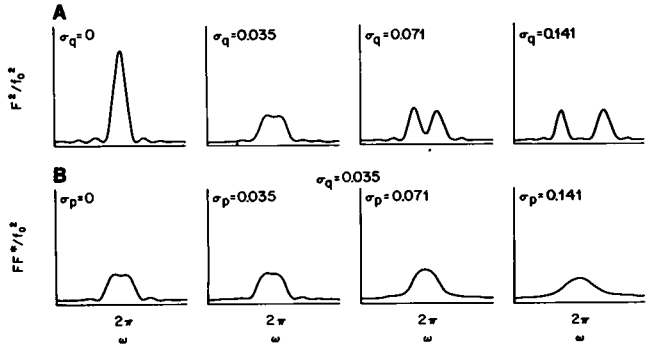

FIGURE 5 First-order diffraction peaks of $\langle |F| \rangle^2 / f_0^2$ computed using Eq. 31 for serial domains in myofibrils. Each myofibril is taken to contain two contiguous domains with (*A*) given by the length distribution of Fig. 2 *D* and with (*B*) given by the length distribution of Fig. 2 *E*. The abscissa contains values of the Fourier variable $\omega = S_x L_0$ in the vicinity of $\omega = 2\Pi$.

Diffraction by a Random Length Sarcomere Array

If the sarcomeres having distributed lengths are randomly placed relative to each other, then Eqs. 20 and 21 show that diffraction peak amplitude decreases, and peak width increases with increasing standard deviation of the length population. Exponentiation of the average value of the phase terms as described by Eqs. 25–27 results in the product of trigonometric terms being replaced by a gaussian exponential term. This term does not vary periodically with Fourier variable ω. Thus any fluctuations in phase arising from the presence of more than one sarcomere length subpopulation or asymmetry of the length distribution are damped out. Thus, these terms contribute no phase angle to the sums of trigonometric functions in Eqs. 20 and 21. Consequently, neither subpeaks nor asymmetry of the diffraction peaks are present. The only information available in the diffraction pattern is the average value of the sarcomere length and the standard deviation of the length distribution. The mathematical form or shape of the length distribution cannot be obtained. This feature and the changes in both diffraction peak amplitude and width occurring with increasing standard deviation of the length distribution result from that feature of the model of the sarcomere array for which the relative position of each sarcomere depends on the lengths of all intervening sarcomeres either within the same myofibril or in different ones. It is this feature which introduces the gaussian term in Eq. 27 as a coefficient in each term of the sums of Eqs.

20 and 21. This coefficient causes both the widening of the diffraction peak and the decrease of its amplitude. The relationship between peak widening and the dependence of the relative position of sarcomeres on the lengths of intervening ones is not as immediately evident in the equation relating the peak width and standard deviation of length distribution given by Kawai and Kuntz (Eq. 3 in reference 2). In their derivation, the dependence on the relative positions of sarcomeres enters, as shown in their Eq. 5, through the convolution of the sarcomere length distribution function with the gaussian intensity function of the incident laser beam when the radial dependence of the intensity is expressed in units of sarcomere length (their Eqs. 6). The result of fluctuations in sarcomere length is that fluctuating numbers of sarcomeres are illuminated by the incident light and, thus, contribute to the convolution.

Computer-based calculations using Eqs. 20 and 21 show that for length distributions with a standard deviation exceeding 0.16 and 0.33 of the mean length respectively, the amplitudes of the first-order peaks in contributions made by the average pair of myofibrils $\langle F \rangle \langle F^* \rangle$ and single myofibril $\langle |F|^2 \rangle$ are <1% of the height of the zeroeth order peaks and, thus, of questionable detectability. Computations of the standard deviation of the sarcomeres length distribution form the width of the first-order diffraction peak of striated muscle (2, 7, 22) under physiological conditions give values of $\sigma \leqq 0.1\ L_0$. Therefore, in muscle diffraction experiments, the presence of severely reduced detectability due to a large value of standard deviation appears unlikely.

Diffraction by Sarcomere Domains

If domains of saromeres, each containing serial contiguous sarcomeres of the same length subpopulation, are present, and if the distribution function describing the entire sarcomere length population is discrete with at least two subpopulations present, then Eqs. 28, 30, and 31 show that subpeaks are present. Both of these two conditions are necessary for subpeaks to appear in the meridional diffraction pattern. The equations show that the subpeaks are formed because the individual domains behave as independently diffracting arrays of sarcomeres. The intensity contributions from light diffracted by sarcomeres in two different domains, q and q', are present as peaks located at a position corresponding to the population weighted mean of L_{0q} and $L_{0q'}$. The amplitudes of these contributions or peaks decrease with increasing difference between the characteristic mean lengths. Results of computer-based computations (Fig. 5) made using discrete Dirac delta subpopulations (shown in Fig. 2) illustrate that the peak intensity due to cross terms between the two subpopulations is essentially zero for values of L_{0q} and $L_{0q'}$. For the associated K_q and $K_{q'}$ sarcomeres in each domain such that the equation

$$L_{0q} \leqq L_{0q'} \left(\frac{K_{q'}}{K_q}\right)\left(\frac{K_q - 1}{K_q + 1}\right) \tag{35}$$

is satisfied, the discrete subpeaks arising independently from domains q and q' are entirely separated. This is because Eq. 35 also specifies the condition for which the first diffraction minimum adjacent to each diffraction maximum coincides in position. Clearly, as the values of the K_q increase, this distance decreases and approaches zero for very large values.

Examination of Eqs. 28, 29, and 32 reveals that the distance between diffraction peaks scales directly with the reciprocal of their associated L_{0q}, and the number of subpopulations present is equal to the number of discrete diffraction peaks. Under the conditions of Eq. 35, the relative amplitudes of each of the q subpeaks due to the average myofibril, scale with the population number fraction g_q. The relative amplitudes of those due to the average pair of myofibrils scale as g_q^2.

If the sarcomeres within domains have distributed lengths δL_q about the mean values L_{0q}, and the placement of sarcomeres within each domain is entirely random, then Eqs. 28, 29, and 32 show that subpeak height decreases and subpeak width increases. Eq. 20 for the average myofibril (with substitution of K_q and L_{0q} for $2J$ and L_0, respectively) describes the effect on subpeak shape of increasing standard deviation σ_q. The double sums in Eqs. 29 and 32 describe diffraction from sarcomeres in different domains, for the case in which each domain q and q' is characterized by having fluctuations δL_q about the mean L_{0q}, and standard deviation σ_q. Computer studies of these sums show that with increasing values of σ^2, the amplitude of the peak present at the population fraction weighed mean of L_{0q} and $L_{0q'}$ decreases. Also the value of the difference between L_{0q} and $L_{0q'}$, for which its amplitude is negligible, decreases with increasing σ_q and $\sigma_{q'}$.

Applications to Diffraction Patterns with Subpeaks

In the following article, Tameyasu et al. (23) have used distances between subpeak maxima as a measure of the differences between the values of mean lengths of sarcomeres subpopulations. Eqs. 28, 29, and 32 of this paper provide a physical basis for their measurements.

Applications to Zeroeth Order Peak Shape

Analysis of equations describing the contributions to the meridional diffracted light intensity by the average myofibril and the average pair of myofibrils in the vicinity of the Fourier parameter $\omega = 0$ shows the shape of the zeroeth order diffraction peak. Computer-generated plots obtained with Eqs. 20 and 21 and 28 and 29 show that the zeroeth order peak for both $\langle |F|^2 \rangle$ and $\langle F \rangle \langle F^* \rangle$ (in the cases of

diffraction by a random array of sarcomeres with distributed length and by an array in which each individual myofibril comprises a domain) decreases monotonically to zero. However, studies to date for the case in which three or more serial sarcomere domains, each having distributed sarcomere lengths about the mean, make up each myofibril, show that the amplitude of the zeroeth order peak is modulated by a higher frequency (or longer period) term in the region of $\omega = 0$. The result of this modulation is subpeaks residing on the flank of the zeroeth order peak. Analysis of Eqs. 31 and 32 shows that the modulation term arises from constructive light interference between pairs of domains separated by intervening ones with the period scaling with the number of intervening sarcomeres. The foregoing observations suggest that subpeaks previously observed in the vicinity of the zeroeth order peak (10) may arise from the presence of sarcomere domains as well as from effect of sample cross-sectional shape as noted previously (10).

Effects of Lateral Myofibrillar Arrangement upon Diffraction

We have considered a volume of myofibrils in which the lengths of all sarcomeres are described by the same distribution function $H(L)$. Effects of lateral clustering of myofibrils according to sarcomere subpopulation has not been considered. Current optical diffraction and direct image studies in our laboratory on thin sections of skeletal muscle, which were fixed at rest length and stained, suggest that myofibrillar regions are typified by a homogeneous length distribution which occupies significant volumes of striated muscle. However, a generalization of these results may be particularly useful in analysis of diffraction patterns obtained from heart muscle where individual cells have been noted to possess unique lengths (24). Thus, study of a multicellular cardiac muscle preparation will generally involve diffraction by an array of myofibrils containing more than one region with a homogeneous length distribution. Consider two such regions to be present in a volume defined by $[MN(2J)]$ and $[M'N'(2J)]$. The present equations derived for the average myofibril describe the contribution $\langle |F|^2 \rangle$ and $\langle |F'|^2 \rangle$ to meridional light intensity. Those derived for the average pair of myofibrils describe $\langle F \rangle \langle F^* \rangle$ and $\langle F' \rangle \langle F'^* \rangle$. These equations with weighting by the exponential term in Eq. 15, and when summed appropriately over m, n and m', n', describe the meridional component of light density diffracted by the average pair of myofibrils, lying, respectively, entirely within MN or $M'N'$. If there is no z-plate misregistry present, then this contribution lies along the meridional axis. Diffraction effects between a pair of myofibrils, each lying in one of the different regions, are given by $\langle F^*_{mn} \rangle \langle F_{m'n'} \rangle$ and its complex conjugate, with each multiplied by the complex exponential in the equation. This multiplication introduces a phase angle $[(mn - m'n')(Y + Z) + \Delta Z_{mn} - \Delta Z_{m'n'}]$ into the argument of each trigonometric term in the product $\langle F^*_{mn} \rangle \langle F_{m'n'} \rangle$ and its complex conjugate. Thus, these terms contribute to the off meridional axis light intensity. This intensity as well as that contributed by scattering from a pair of myofibrils lying entirely within each region, may be negligible relative to individual contribution from the individual regions if differences between mean values of sarcomere length and values of subpopulation standard deviation are sufficiently large, as discussed above.

We are currently applying the equations derived in this work, those of Yeh and co-workers describing effects of fluctuating and linear z-disk misalignment and our equations describing effects of wavey z-disk contours (19) towards the analysis of the light diffraction patterns obtained in our laboratory from fixed and stained thin sections of striated muscle which have a homogeneous $H(L)$. In this preparation z-disk misalignment and lateral spacing need be considered in only one dimension in analyses during Eqs. 16–34.

In these preparations, the results of our previous measurements and calculations (19) show that the effect of the z-disk misregistry is to move and modulate the intensities of the meridional diffraction peaks in an equatorial direction according to the symmetry and shape of the misregistry contour about the longitudinal myofibrillar axis. The z-disk misregistry does not cause movement of peaks or splitting of subpeaks in the meridional direction as shown in our measurements and calculations.

We also currently are examining diffraction patterns obtained from regions of thin sections of striated muscle which contain areas having different sarcomere length populations to determine the dependence of contributions to diffracted light intensity by wave interferences of light diffracted by sarcomeres in the different regions upon differences between the values of mean length and standard deviation of the populations.

Diffraction and light scattering by structures in muscle other than sarcomeres and optical effects stemming from the gaussian intensity profile of the laser beam might be expected to mimic diffraction by an array of sarcomeres with discrete lengths. Pollack and Krueger (25) have suggested that the widening of the zeroeth order light diffraction peak of striated muscle is due to light scattering by mitochondria, sarcoplasmic reticulum and nuclei. In support of this idea, light-turbidity measurements, in which the changes in transmitted light are due to scattering away from the incident direction, have been used to detect changes in the shape, and hence the metabolic state, of mitochondria (26).

Treating the array of mitochondria as oriented rods with aperiodic spacing and widely dispersed lengths (27) we have derived an equation describing the scattering of the zeroeth order peak by these structures. Because of the lack of periodicity the array behaves as a group of independent light scatterers with no constructive wave interfer-

ences or diffraction effects. The effect of dispersion of the length L of the mitochondrion upon averaging is to smooth out the lobes of light intensity in the scattering function $\sin^2(SL)/(SL)^2$ for the individual mitochondrion so that the intensity of light scattered by the mitochondria monotonically decreases in gaussian-like fashion in directions away from that of the incident light. This result supports the suggestion of Pollack and Krueger (25). Because mitochondria comprise the majority of the extrasarcomeric volume in the cat (28) with the sarcoplasmic reticulum and nuclei occupying only a small volume fraction, little, if any, perturbation by these structures of the light diffracted by sarcomeres is expected.

Yeh and co-workers (12) have pointed out that the thickness of the muscle preparation leads to multiple scattering of the initially diffracted beams. The fundamental equations of multiple scattering (29) show that light intensity is exchanged between major diffraction peaks and that no new peaks arise from this process. Although relative intensities of mth order peaks are altered, the ratios between the amplitude of subpeaks of the same order and their spacing which are present in patterns from myofibrils containing sarcomere domains are not changed by multiple scattering.

The light intensity of a gaussian laser beam decreases monotonically with distance from the center. Substitution of a gaussian light intensity function into Eqs. 18 and 19 shows that the resulting diffraction pattern of the sarcomere array has no additional peaks. The effect is to widen and decrease the amplitude of the major order diffraction peaks and subpeaks, and secondary diffraction maxima.

This research was supported in part by an Ischemic Specialized Center of Research (SCOR) Grant HL 17669-07 and the National Aeronautic and Space Administration Contract NAS 210354.

Received for publication 5 June 1981 and in revised form 5 October 1981.

REFERENCES

1. Cleworth, D. R., and K. A. P. Edman. 1971. Changes in sarcomere length during isometric tension development in frog skeletal muscle. *J. Physiol. (Lond.).* 227:1–17.
2. Kawai, M., and I. D. Kuntz. 1973. Optical diffraction studies of muscle fibers. *Biophys. J.* 13:857–876.
3. Nasser, R., A. Manring, and E. A. Johnson. 1974. Light diffraction of cardiac muscle: sarcomere motion during contraction. *In* The Physiological Basis of Starling's Law of the Heart *Ciba Found. Symp.* 57–81.
4. Umazume, Y., and S. Fujime. 1975. Electro-optical property of extremely stretched skinned muscle fibers. *Biophys. J.* 15:163–180.
5. Paolini, P. J., and K. P. Roos. 1975. Length-dependent optical diffraction pattern changes in frog sartorius muscle. *Physiol. Chem. Physics.* 7:235–254.
6. Pollack, G., T. Iwazumi, H. E. D. J. Ter Keurs, and E. F. Shibata. 1977. Sarcomere shortening in striated muscles occurs in stepwise fashion. *Nature (Lond.).* 268:757–759.
7. Paolini, P. J., R. Sabbadini, K. P. Roos, and R. J. Baskin. 1976. Sarcomere length dispersion in single skeletal muscle fibers and fiber bundles. *Biophys. J.* 16:919–930.
8. Rudel, R., and F. Zite-Ferenczy. 1977. Intensity behaviour of light diffracted by single frog muscle fibers from narrow laser beams. *J. Physiol. (Lond.).* 272:31–32P.
9. Rudel, R., and F. Zite-Ferenczy. 1979. Interpretation of light diffraction by cross-striated muscle as Bragg reflection of light by the lattice of contractile proteins. *J. Physiol. (Lond.).* 290:317–319.
10. Krueger, J. W., D. Forletti, and B. A. Wittenberg. 1980. Uniform sarcomere shortening behavior in isolated cardiac muscle cells. *J. Gen. Physiol.* 76:587–607.
11. Huxley, H. E., and J. Hanson. 1957. Quantitative studies on the structure of cross-striated myofibrils. I. Investigations by interference microscopy. *Biochim. Biophys. Acta.* 23:229–249.
12. Yeh, Y., R. J. Baskin, R. L. Lieber, and K. P. Roos. 1980. Theory of light diffraction by single skeletal muscle fibers. *Biophys. J.* 29:509–522.
13. Gaskill, J. D. 1978. Linear Systems, Fourier Transforms, and Optics. John Wiley and Sons, Inc., New York. 375–385.
14. Morse, P. M., and H. Feshbach. 1953. Methods of Theoretical Physics, Part II. McGraw-Hill Book Company, New York. 1073.
15. Fujime, S., and S. Yoshino. 1978. Optical diffraction study of muscle fibers. I. A theoretical basss. *Biophys. Chem.* 8:305–315.
16. Baskin, R. J., K. P. Roos, and Y. Yeh. 1979. Light diffraction study of single skeletal muscle fibers. *Biophys. J.* 28:45–64.
17. Bear, R. S., and D. E. A. Bolduan. 1950. Diffraction by cylindrical bodies with periodic axial structure. *Acta Cryst. Allogr. Sect. B. Struct. Crystallogr. Chem.* 3:236–241.
18. Born, M., and E. Wolf. 1975. Principles of Optics. Pergamon Press, New York. 401–405.
19. Judy, M. M., V. Summerour, T. L. LeConey, and G. H. Templeton. 1980. Effects of z-plate mis-registry on optical diffraction by striated muscle. *Biophys. J. (Abstr.).* 33:22*a*.
20. Gaskill, J. D. 1978. Linear Systems, Fourier Transforms, and Optics. John Wiley and Sons, Inc., New York, p. 111.
21. Papoulis, A. 1965. Probability, Random Processes, and Stochastic Processes. McGraw-Hill Book Company, New York. 266–267.
22. Ter Keurs, H. E. D. J., T. Iwazumi, and G. H. Pollack. 1978. The sarcomere length-tension relation in skeletal muscle. *J. Gen. Physiol.* 72:565–592.
23. Tameyasu, T., N. Ishide, and G. H. Pollack. 1981. Discrete sarcomere length distributions in skeletal muscle. *Biophys. J.* 37:489–492.
24. Winegrad, S. 1974. Functional implications of the resting sarcomere length-tension curve in living heart muscle. *In* The Physiological Basis of Starling's Law of the Heart *Ciba Found. Symp.* 43–55.
25. Pollack, G., and J. W. Krueger. 1976. Sarcomere dynamics in intact cardiac muscle. *Eur. J. Cardiol.* 4 (Suppl.):53–65.
26. Sordahl, L. A., C. Johnson, Z. R. Blailock, and A. Schwartz. 1971. The mitochondrion. *Methods Pharmacol.* 1:247–286.
27. Page, E. 1978. Quantitative ultrastructural analysis in cardiac membrane physiology. *Am. J. Physiol.* 235:C147–C158.
28. Page, E., and H. A. Fozzard. 1973. Capacitive, resistive and syncytial properties of heart muscle: Ultrastructural and physiological considerations. *In* Structure and Function of Muscle. G. H. Bourne, editor. Academic Press, Inc., New York, 2 (second edition):91–158.
29. Korpel, A. 1981. Acousto-optics: a review of fundamentals. *Proc. I.E.E.* 69:48–53.